Scientific Research Publishing

Journal of Applied Mathematics and Physics, 2026, 14(11), 4793-4818
https://www.scirp.org/journal/jamp
ISSN Online: 2327-4379
ISSN Print: 2327-4352

Biorthogonal Spline-Wavelet Transfers: An L^2 Criterion, a Rational Construction, and a Minimal-Mask Obstruction

Mehmet Ersoy

Institut de Mathématiques de Toulon (IMATH), Université de Toulon, Toulon, France
Email: mailto:mehmet.ersoy@univ-tln.fr, mehmet.ersoy@univ-tln.fr

How to cite this paper: Ersoy, M. (2026) Biorthogonal Spline-Wavelet Transfers: An L^2 Criterion, a Rational Construction, and a Minimal-Mask Obstruction. *Journal of Applied Mathematics and Physics*, **14**, 4793-4818.
https://doi.org/10.4236/jamp.2026.1411234

Received: October 14, 2026
Accepted: November 23, 2026
Published: November 26, 2026

Copyright © 2026 by author(s) and Scientific Research Publishing Inc.
This work is licensed under the Creative Commons Attribution International License (CC BY 4.0).
http://creativecommons.org/licenses/by/4.0/

Open Access

Abstract

An earlier construction proposed transferring a cardinal B-spline factor between the members of a biorthogonal scaling pair. The inverse box convolution is unbounded on L^2 and requires an input condition. For compactly supported data, we prove equivalent Fourier, Sobolev, and local-moment tests for its L^2 existence and a finite inverse formula. For a certified biorthogonal seed, we derive translate Riesz bounds. We then give an explicit rational order-four spline seed with a 19-position dual filter. An exact Bernstein certificate proves the dual scaling function belongs to H^1; a finite correlation rank witness establishes functional biorthogonality, and rational Gram bounds yield the transferred pair's squared-norm translate constants 1/48 and 48. A strict Fourier-decay bound and the Cohen-Daubechies-Feauveau cross-scale criterion prove dual Riesz wavelet bases of $L^2(\mathbb{R})$. This coefficient choice repairs a failure of the degree-minimal symmetric complement: we prove its unique algebraic mask has no compactly supported L^2 dual for every spline order $m \geq 4$. The order-four filters alone therefore give a counterexample to inferring functions from perfect reconstruction. Daubechies $D8$ and $D24$ seeds give further certified transfers, including full-scale wavelet bases. The spline transfer, Bézout construction, and general cross-scale criterion have precedents in He and Cohen-Daubechies-Feauveau; our claims concern the stated inverse-domain characterization, explicit rational design and certificates, and uniform obstruction within the specified minimal class.

Keywords

Biorthogonal Wavelets, B-Spline Convolution, Refinement Masks, Riesz Bounds, Sobolev Regularity

1. Introduction

Let $b = \mathbf{1}_{[0,1]}$ and define box convolution and its adjoint by

$$Tf(x) = \int_{x-1}^{x} f(y)\,\mathrm{d}y = b * f(x), \quad T^{*} f(x) = \int_{x}^{x+1} f(y)\,\mathrm{d}y. \tag{1}$$

The aim of the author's note [1] was to construct new biorthogonal wavelets *from an initial pair*. For a compactly supported biorthogonal scaling pair $(\phi, \tilde{\phi})$ it proposed the factor transfer

$$\Phi_s = T^s \phi, \quad \tilde{\Phi}_s = \left(T^{*}\right)^{-s} \tilde{\phi}, \quad s \in \mathbb{N}^{*}. \tag{2}$$

The 2009 note [1] also gave recurrences for the new finite filters. The scaling curves in its figures are illustrations of the procedure, not inputs that must be reverse engineered before it can be used. Given *any specified admissible seed*, the filter recurrences determine new filters; the original plotted seed coefficients would be needed only to reproduce those particular curves exactly. Adjunction gives the desired translate biorthogonality only when $\tilde{\Phi}_s$ exists in L^2. A perfect-reconstruction identity for finite filters does not guarantee that existence.

Spline-factor transfers and differentiation identities have precedents in Cohen, Daubechies and Feauveau [2], Lemarié-Rieusset [3], and Unser and Blu [4]. The classical compact spline factorizations and shortened supports are studied by Ron [5] and Plonka and Ron [6]; Strang-Fix zeros and spline division alone are not claimed as discoveries here. He [7] [8] explicitly treats spline convolution, its dual inverse, sufficient L^2 conditions and initial biorthogonal pairs. In particular, ([8], Theorems 3.4-3.5) states a coefficient-based sufficient criterion for the dual L^2 function and performs the transfer from a biorthogonal seed. The operation (2) and its classical spline descendants are therefore not presented as a new wavelet family. This paper puts the 2009 *construction procedure* [1] on a precise functional footing: it characterizes the inverse domain for *every* compactly supported L^2 input, independently of a refinement mask or a sufficient coefficient inequality, gives a pointwise finite local-moment test, establishes a finite formula and translate Riesz bounds, states when the resulting wavelets are globally stable, and identifies an entire degree-minimal mask class with an L^2 obstruction from order four onward. We additionally give a particular rational extension of that minimal mask that restores L^2 existence and yields an explicit dual wavelet basis with certified bounds. Section 4.1 assembles the results into a reproducible procedure.

Result-by-Result Comparison with Prior Work

The labels in **Table 1** refer to statements in this paper; the comparison is about their *logical content*, not their notation. He (2004) already states the spline transfer for an initial biorthogonal pair, and He (2007), Theorems 3.4-3.5, gives explicit sufficient coefficient conditions. CDF's Theorem 3.8 already gives the full-scale dual Riesz-basis conclusion once its decay and scaling-function biorthogonality hypotheses hold. Neither construction is claimed as new here. Ron and Plonka-Ron already factor compactly supported refinable functions into B-spline and

compactly supported distributional factors; our range theorem isolates the L^2 requirement and quantitative inverse for the adjoint box operator. For the degree-minimal symmetric spline complement, CDF already gave the Bézout construction and used the $2\pi/3$ cycle in its spline analysis ([2], Section 6.A); a further time-domain characterization is in Bittner [9]. Dijkema ([10], Table 2.1) reports negative Sobolev regularity for the symmetric m/m duals at $m = 4, \cdots, 20$. Our Theorem 10 supplies a short exact proof of the obstruction *uniformly* for all $m \geq 4$; neither the algebraic masks nor the order-four observation are claimed as new.

Table 1. Statement-by-statement relation to He (2004, 2007) and CDF (1992).

Statement here	Precedent in He [7] [8]	Precedent in CDF [2] and precise role here
Propositions 2.1-2.2	Inverses need not be L^2 functions; He (2007), Section 3, explicitly allows distributional partners.	Section 1.C warns that filter reconstruction need not yield a functional basis. Here the L^2 range obstruction is made explicit.
Theorem 2.3	He (2007), Theorem 3.4, gives a *sufficient* inequality on the coefficients of a factored refinable mask. The present equivalence applies to any compact $f \in L^2$, even without a mask; Ron (1990) and Plonka-Ron (2001) supply general compact spline factorizations.	Sections 3-4 analyze refinable Fourier products; the finite local moments and two-sided estimates here concern the L^2 inverse of the specific box-adjoint operator.
Theorem 3.1 and Corollary 3.2	He (2007), Theorem 3.5, already constructs transferred biorthogonal pairs with its coefficient condition.	Section 6.A already contains spline-derived pairs. Here the exact input condition yields explicit *single-scale* translate constants.
Proposition 4.1 and Corollary 4.2	He (2004, 2007) derives finite filter transfers and sum-rule changes.	Sections 2 and 4 separate perfect reconstruction from functional existence. Here divisibility *and* H^s are jointly necessary and sufficient for the inverse of a known compact seed.
Statement here	Precedent in He [7] [8]	Precedent in CDF [2] and precise role here
Procedure 4.1	The 2009 note [1] and He (2004, 2007) contain the factor-transfer procedure.	This implementation adds exact input checks, a finite derivative inverse, and separate statements for masks, functions, translate bounds and cross-scale stability.
Theorem 4.3	Transferred spline-type wavelets already appear in He.	Theorem 3.8 supplies the cross-scale result. Here its hypotheses are checked for *D*24 by the finite rational certificate (28).
Theorem 7.1	He's coefficient conditions give other sufficient constructions; this rational mask and its finite exact certificate are specified here.	CDF supplies the free Bézout family and the cross-scale criterion; our choice R in (41), L^2 proof, correlation-rank witness, and rational Riesz constants are explicit.
Theorem 6.1 and Proposition 6.2	Distributional inverse partners are already discussed by He (2007).	Failure of a filter-only inference is known. Here a uniquely specified degree-minimal symmetric spline-mask class fails to yield compact L^2 duals for all orders $m \geq 4$; $m = 4$ gives exact taps.

2. The Inverse Domain

Use the Fourier convention $\hat{f}(\xi)=\int_{\mathbb{R}} f(x)\mathrm{e}^{-\mathrm{i}x\xi}\mathrm{d}x$. The multipliers of T and T^* are

$$\tau(\xi)=\frac{1-\mathrm{e}^{-\mathrm{i}\xi}}{\mathrm{i}\xi},\quad \tau_{-}(\xi)=\frac{\mathrm{e}^{\mathrm{i}\xi}-1}{\mathrm{i}\xi}, \tag{3}$$

extended by 1 at $\xi=0$.

Proposition 2.1. The operators T,T^* are bounded and injective on $L^2(\mathbb{R})$, have dense nonclosed ranges, are not compact, and have unbounded inverses on their ranges.

Proof. Young gives $\|T\|,\|T^*\|\le 1$. Their multipliers vanish only on $2\pi\mathbb{Z}\setminus\{0\}$, so both operators and their adjoints have trivial kernels; their ranges are dense. Unit-norm Fourier data concentrated near 2π have output norm tending to zero. The inverses are unbounded and the ranges nonclosed. Widely separated translates of a nonzero compactly supported input have outputs with equal nonzero norm and disjoint supports; hence the operators are not compact. □

Proposition 2.2. (Haar obstruction) The Haar scaling function b is not in $\mathrm{Ran}\left(T^*\big|_{L^2}\right)$.

Proof. For $g\in L^2$, $\left(T^*g\right)'=g(\cdot+1)-g\in L^2$, whereas $b'=\delta_0-\delta_1\notin L^2$. □

Theorem 2.3 (compactly supported inverse criterion). Let $s\ge 1$ and $f\in L^2(\mathbb{R})$ have support in $[a,b]$. The following are equivalent:

1) there is $g\in L^2$ satisfying $\left(T^*\right)^s g=f$;

2) $f\in H^s(\mathbb{R})$ and $\hat{f}$ has a zero of order at least s at each $2\pi n$, $n\in\mathbb{Z}\setminus\{0\}$;

3) $\hat{f}/\tau_{-}^{s}\in L^2$, defined almost everywhere.

4) $f\in H^s(\mathbb{R})$ and, for almost every $t\in[0,1)$,

$$\sum_{j\in\mathbb{Z}} j^r f^{(s)}(t+j)=0,\quad r=0,\cdots,s-1. \tag{4}$$

Each sum has finitely many nonzero terms.

In this case g is unique, supported in $[a+s,b]$, and equals

$$g(x)=\sum_{k=s}^{\infty}\binom{k-1}{s-1}f^{(s)}(x-k)\quad \text{a.e.} \tag{5}$$

With $K=\lceil b-a\rceil$ and $\binom{K}{s}=0$ for $K<s$,

$$2^{-s}\left\|f^{(s)}\right\|_2\le\|g\|_2\le\binom{K}{s}\left\|f^{(s)}\right\|_2. \tag{6}$$

Proof. Plancherel and the almost-everywhere nonvanishing of τ_{-} give (i) ⇔ (iii). If (i) holds, write $Eg(x)=g(x+1)$ and $F=f^{(s)}$. Then

$$F=D^s\left(T^*\right)^s g=(E-I)^s g\in L^2. \tag{7}$$

Put $u_j(t)=g(t+j)$. Fubini gives

$$\int_0^1 \sum_{j\in\mathbb{Z}} \left|u_j(t)\right|^2 \mathrm{d}t = \|g\|_2^2,$$

so $u(t)\in \ell^2(\mathbb{Z})$ for almost every $t\in[0,1)$. After intersecting countably many full-measure sets, the identity $(E-I)^s u_j(t)=F(t+j)$ holds for every j on one common full-measure set of such t; here E shifts the sequence index by one. Since $\operatorname{supp} F\subset[a,b]$, the fixed integers

$$J_-=\lfloor a\rfloor - s - 1, \quad J_+=\lceil b\rceil + 1$$

satisfy $F(t+j)=0$ whenever $j\le J_-$ or $j\ge J_+$, uniformly for $0\le t<1$ outside this null set. The homogeneous recurrence makes $u_j(t)$ a polynomial in j of degree at most $s-1$ on each of these tails. A polynomial tail in ℓ^2 is identically zero. Thus the indices beyond which $u_j(t)=0$ can be chosen independently of t, and g vanishes outside a fixed compact interval. This proves compactness; the sharper support interval $[a+s,b]$ is obtained below from (5). Because $\hat{f}=\tau_-^s\hat{g}$ and Fourier transforms of compact L^2 functions are entire, (ii) follows.

Assume (ii). The function $\hat{F}(\xi)=(\mathrm{i}\xi)^s\hat{f}(\xi)$ has zeros of order s at all $2\pi n$, including $n=0$. For each $0\le m<s$, the periodization $Q_m(t)=\sum_{j\in\mathbb{Z}}(t+j)^m F(t+j)$ belongs to $L^2(0,1)$, since F is compactly supported. Its nth Fourier coefficient is

$$\int_0^1 Q_m(t)\mathrm{e}^{-2\pi\mathrm{i}nt}\mathrm{d}t=\int_{\mathbb{R}} x^m F(x)\mathrm{e}^{-2\pi\mathrm{i}nx}\mathrm{d}x=\mathrm{i}^m\hat{F}^{(m)}(2\pi n)=0. \tag{8}$$

Thus $Q_m=0$ almost everywhere. Expanding $j^r=\big((t+j)-t\big)^r$ in terms of the Q_m gives

$$\sum_{j\in\mathbb{Z}} j^r F(t+j)=0 \quad \text{for a.e. } t\in[0,1), \quad 0\le r<s. \tag{9}$$

This proves (ii) $\Rightarrow$ (iv). Conversely, the identity $(t+j)^m=\sum_{r=0}^m \binom{m}{r} t^{m-r}j^r$ shows that (iv) annihilates every Q_m. Its Fourier coefficients in (8) give $\hat{F}^{(m)}(2\pi n)=0$ for $m<s$; at nonzero $2\pi n$ this is equivalent to a zero of order s of $\hat{f}$. Hence (iv) $\Rightarrow$ (ii). Define g by (5). It vanishes for $x<a+s$. For $x>b$, the coefficient $\binom{k-1}{s-1}$ is a polynomial of degree $s-1$ in k, so (9) annuls the full sum over $k\in\mathbb{Z}$. Terms $k\le 0$ vanish by support and $1\le k<s$ by their binomial coefficients. Thus $\operatorname{supp} g\subset[a+s,b]$, and only $s\le k\le K$ contribute there. Translation invariance and $\sum_{k=s}^K \binom{k-1}{s-1}=\binom{K}{s}$ give the upper bound. Finite differences give $(E-I)^s g=F$. By (7), $D^s\left(f-\left(T^*\right)^s g\right)=0$; a compactly supported polynomial distribution is zero. Injectivity gives uniqueness; $\left\|(E-I)^s g\right\|_2\le 2^s\|g\|_2$ gives the lower bound. □

Remark 2.4. Condition (iii) is exact without compact support. Compact support makes the local condition (iv), finite formula and estimates possible.

3. Biorthogonality and Riesz Stability

For compactly supported $u \in L^2$ let

$$B(u) = \sum_{m\in\mathbb{Z}} \left| u, u(\cdot - m) \right| < \infty. \tag{10}$$

Theorem 3.1. (domain transfer). Let $(\phi, \tilde{\phi})$ be a compactly supported L^2 biorthogonal scaling pair with finite real refinement masks, normalized by $\int \phi = \int \tilde{\phi} = 1$. Suppose $\tilde{\phi}$ satisfies Theorem 3(ii) for some $s \geq 1$. Then both functions in (2) are compactly supported L^2 functions and

$$\left\langle \Phi_s(\cdot - k), \tilde{\Phi}_s(\cdot - l) \right\rangle = \delta_{kl}. \tag{11}$$

For every finitely supported sequence c,

$$\frac{\|c\|_{\ell^2}^2}{B(\tilde{\Phi}_s)} \leq \left\| \sum_k c_k \Phi_s(\cdot - k) \right\|_2^2 \leq B(\Phi_s) \|c\|_{\ell^2}^2, \tag{12}$$

$$\frac{\|c\|_{\ell^2}^2}{B(\Phi_s)} \leq \left\| \sum_k c_k \tilde{\Phi}_s(\cdot - k) \right\|_2^2 \leq B(\tilde{\Phi}_s) \|c\|_{\ell^2}^2.$$

Proof. Theorem 3 gives the inverse in L^2; Young gives $\Phi_s \in L^2$. Adjunction and translation commutation give (11). The translate Gram matrix is convolution by the finitely supported correlation sequence of each function; Young on ℓ^2 gives the upper constants B. If $U = \sum c_k \Phi_s(\cdot - k)$, then biorthogonality and Cauchy-Schwarz yield $\|c\|_{\ell^2}^2 \leq \|U\|_2 \sqrt{B(\tilde{\Phi}_s)} \|c\|_{\ell^2}$. The opposite lower bound is symmetric. □

Corollary 3.2 (computable geometric bounds). If $\operatorname{supp}\phi \subset [a,b]$ and $\operatorname{supp}\tilde{\phi} \subset [c,d]$, put $L = b - a$, $\tilde{L} = d - c$, $K = \lceil \tilde{L} \rceil$, $N(t) = 2\lceil t \rceil + 1$. The upper constants in (12) can be replaced by

$$B_\Phi = N(L+s) \|\phi\|_2^2, \quad B_{\tilde{\Phi}} = N(\tilde{L} - s) \binom{K}{s}^2 \left\| \tilde{\phi}^{(s)} \right\|_2^2. \tag{13}$$

Their reciprocals on the opposite sides are lower constants.

Proof. The support intervals are $[a, b+s]$ and $[c+s, d]$. At most $N(t)$ correlations of an interval-supported function of length t are nonzero, each bounded by its squared norm. Apply (6). □

4. The Mask Test and the Wavelet Scope

Write the refinement masks as $H(z) = \frac{1}{2}\sum_k h_k z^k$ and $\tilde{H}(z) = \frac{1}{2}\sum_k \tilde{h}_k z^k$, and set $A(z) = (1+z)/2$. Both masks equal 1 at 1. The multiplier ratios in (3) imply

$$H_s(z) = H(z) A(z)^s, \quad \tilde{H}_s(z) = \tilde{H}(z) \left(\frac{z}{A(z)} \right)^s. \tag{14}$$

Equating coefficients gives the constructive recurrence of the 2009 note [1], written in the present adjoint and mask convention:

$$h_k^{(s)} = 2^{-s}\sum_{\ell=0}^{s}\binom{s}{\ell}h_{k-\ell}, \tag{15}$$

$$\sum_{\ell=0}^{s}\binom{s}{\ell}\tilde{h}_{k-\ell}^{(s)} = 2^s\tilde{h}_{k-s}.$$

The shift on the right records the choice of T^* and of the coordinate origin. When $(1+z)^s$ divides $\tilde{H}$, exact Laurent-polynomial division determines every dual tap. Thus, the coefficients of a *new* pair are calculable from any specified admissible seed.

Proposition 4.1. Under Theorem 3.1, $(1+z)^s$ divides $\tilde{H}(z)$ in $\mathbb{R}\left[z,z^{-1}\right]$. Thus, the transformed masks are finite and inherit perfect reconstruction.

Proof. Theorem 2.3 says that the seed transform $\hat{\tilde{\phi}}$ vanishes to order s at every nonzero multiple of 2π. The seed has stable translates, so its periodized Fourier Gramian is bounded below almost everywhere. Here $\tilde{\phi}\in H^s$ and its derivatives have compact support, hence $\left|\hat{\tilde{\phi}}(\xi)\right|\le C\left(1+|\xi|\right)^{-s}$. The squared periodization converges uniformly; it is also the continuous trigonometric polynomial of the finitely many translate correlations. Thus, its almost-everywhere lower bound holds at π. In particular, for some integer n, $\hat{\tilde{\phi}}(\pi+2\pi n)\neq 0$. The seed refinement equation $\hat{\tilde{\phi}}(2\omega)=\tilde{H}\left(\mathrm{e}^{-\mathrm{i}\omega}\right)\hat{\tilde{\phi}}(\omega)$ at $\omega=\pi+2\pi n$ therefore forces $\tilde{H}$ to vanish to order s at -1. On the unit circle $A(z)^s\overline{\left(z/A(z)\right)^s}=1$ away from -1; the perfect-reconstruction identity extends by continuity. □

Corollary 4.2 (Sobolev and finite-mask test). Under the seed-pair assumptions, the inverse $\left(T^*\right)^{-s}\tilde{\phi}$ lies in L^2 if and only if

$$\tilde{\phi}\in H^s(\mathbb{R}) \text{ and } (1+z)^s \text{ divides } \tilde{H}(z) \text{ in } \mathbb{R}\left[z,z^{-1}\right]. \tag{16}$$

It is then compactly supported with the Riesz bounds above.

Proof. Necessity follows from (7) and Proposition 4.1. For sufficiency write $n=2^q m$ with m odd for each nonzero integer n. Iterating refinement $q+1$ times gives

$$\hat{\tilde{\phi}}(\xi)=\prod_{r=1}^{q+1}\tilde{H}\left(\mathrm{e}^{-\mathrm{i}\xi/2^r}\right)\hat{\tilde{\phi}}\left(\xi/2^{q+1}\right).$$

At $\xi=2\pi n$ the $r=q+1$ factor is evaluated at -1 and has a zero of order at least s. All remaining factors are analytic near that point because the mask is finite and $\tilde{\phi}$ is compactly supported. Hence the entire product has the required zero order. Theorem 2.3(ii) now applies. □

If the seed masks have zero orders p,q at -1, the new orders are $p+s,q-s$. In particular, $q\ge s+1$ retains a sum rule on both sides.

For real masks, the cross-filters $g_k=(-1)^k\tilde{h}_{1-k}^{(s)}$ and $\tilde{g}_k=(-1)^k h_{1-k}^{(s)}$ define $\Psi_s(x)=\sum_k g_k\Phi_s(2x-k)$ and $\tilde{\Psi}_s(x)=\sum_k\tilde{g}_k\tilde{\Phi}_s(2x-k)$, both compactly

supported in L^2. Perfect reconstruction gives single-scale biorthogonality. The next result supplies the cross-scale argument missing from the 2009 construction.

Theorem 4.3 (global stability under Fourier decay). Assume Theorem 3.1. Suppose both transformed masks vanish at -1 and, for some $\varepsilon > 0$, the two transformed scaling functions satisfy

$$\left|\hat{\Phi}_s(\xi)\right| + \left|\hat{\tilde{\Phi}}_s(\xi)\right| \le C\left(1+|\xi|\right)^{-1/2-\varepsilon}. \tag{17}$$

The mask assumption holds if the seed mask zero orders are at least 1 and $s+1$, respectively. A sufficient condition for (17) is that both seed scaling functions lie in $C_c^{s+1+\delta}(\mathbb{R})$ for some $0<\delta<1$, in the usual Hölder sense. Then the wavelets defined by the cross-filters above generate two dual Riesz bases of $L^2(\mathbb{R})$: for every finite array $(c_{j,k})$ there are $0 < A_s \le B_s < \infty$ with

$$A_s \sum_{j,k} \left|c_{j,k}\right|^2 \le \left\| \sum_{j,k} c_{j,k} 2^{j/2} \Psi_s\left(2^j \cdot - k\right) \right\|_2^2 \le B_s \sum_{j,k} \left|c_{j,k}\right|^2. \tag{18}$$

The analogous assertion holds for the dual wavelets.

Proof. We apply Cohen-Daubechies-Feauveau ([2], Theorem 3.8), with the following verification of its assumptions. Proposition 4.1 gives finite real masks $H_s, \tilde{H}_s$ satisfying perfect reconstruction and $H_s(1) = \tilde{H}_s(1) = 1$. The corresponding refinement coefficients in the convention of CDF are $h_k^{(s)}/\sqrt{2}$ and $\tilde{h}_k^{(s)}/\sqrt{2}$; their low-pass symbols are therefore exactly $H_s\left(\mathrm{e}^{-\mathrm{i}\xi}\right)$ and $\tilde{H}_s\left(\mathrm{e}^{-\mathrm{i}\xi}\right)$. Theorem 3.1 supplies compactly supported L^2 refinable functions with biorthogonal integer translates. Both integrals remain one, since box convolution preserves the integral and $\left(T^*\right)^s \tilde{\Phi}_s = \tilde{\phi}$. Their Fourier transforms are continuous at zero with value one; iteration of refinement identifies them with the normalized infinite products used by CDF, up to its Fourier transform normalization. The assumed zeros at -1 give the required low-pass cancellations, and the cross-filters above are the associated dual high-pass filters. Finally, (17) is precisely the required decay with exponent strictly greater than 1/2. CDF's theorem yields the dual wavelet expansions, and the already established translate biorthogonality yields dual Riesz bases and (18). Thus, the conclusion uses a cross-scale theorem in addition to the translate bounds (12).

For the last assertion, the locally finite inverse sum (5) shows $\tilde{\Phi}_s \in C_c^{1+\delta}$; convolution shows $\Phi_s \in C_c^{1+\delta}$ as well. For a compactly supported $C^{1+\delta}$ function u, integration by parts followed by a finite-difference estimate on its Hölder derivative gives $\left|\hat{u}(\xi)\right| \le C_u\left(1+|\xi|\right)^{-1-\delta}$. □

Lemma 4.4 (regularity of an orthonormal scaling function). Let (ϕ, ψ) be a compactly supported orthonormal multiresolution pair. If $\psi \in C_c^{r,\delta}(\mathbb{R})$, where $r \ge 0$ is an integer and $0 < \delta < 1$, then ϕ has a representative in $C_c^{r,\delta}(\mathbb{R})$.

Proof. Since $\phi \in V_0$ and $V_0 = \oplus_{j<0} W_j$, the expansion

$$\phi = \sum_{j<0} \sum_{k\in\mathbb{Z}} \left\langle \phi, \psi_{j,k} \right\rangle \psi_{j,k}, \quad \psi_{j,k}(x) = 2^{j/2} \psi\left(2^j x - k\right),$$

holds in L^2. For each $j<0$, only a number of indices k bounded inde-

pendently of j have supports meeting $\operatorname{supp}\phi$, because the diameter of $2^j \operatorname{supp}\phi$ is uniformly bounded. For those indices, $\left|\left\langle \phi, \psi_{j,k} \right\rangle\right| \le \|\phi\|_1 \|\psi\|_\infty 2^{j/2}$. For $0 \le m \le r$, $\left\|\psi_{j,k}^{(m)}\right\|_\infty \le C_m 2^{j(m+1/2)}$; also $\left[\psi_{j,k}^{(r)}\right]_{C^{0,\delta}} \le C 2^{j(r+\delta+1/2)}$. Consequently, the expansion converges absolutely in $C^{r,\delta}$, by summing the geometric majorants $2^{j(m+1)}$ and $2^{j(r+\delta+1)}$ over $j<0$. Its limit equals ϕ in L^2 and therefore has the same compact support. □

4.1. Construction from a Specified Seed

The following is the construction proposed in 2009 [1] with its functional checks made explicit. Each step has a separate output and a stated guarantee.

1) **Specify and test the input.** Choose an integer $s \ge 1$ and a *known compactly supported* L^2 *biorthogonal scaling pair* $\left(\phi, \tilde{\phi}\right)$ with normalized finite masks $\left(H, \tilde{H}\right)$. Check $\tilde{\phi} \in H^s$ and exact Laurent divisibility $(1+z)^s \mid \tilde{H}$. Corollary 2 says that these two checks are necessary and sufficient for the compact L^2 inverse. A proposed pair of masks without an independently established L^2 seed is not yet such an input.

2) **Calculate the finite filters.** Apply (15) to obtain $\left(h_k^{(s)}, \tilde{h}_k^{(s)}\right)$, and use the cross-filter formula above to obtain $\left(g_k, \tilde{g}_k\right)$. Proposition 4.1 proves finite support and algebraic perfect reconstruction.

3) **Construct and bound the functions.** Form $\Phi_s = b^{*s} * \phi$ and compute $\tilde{\Phi}_s$ by the finite-on-support derivative sum (5) with $f = \tilde{\phi}$. Theorem 3.1 proves the biorthogonality and positive translate Riesz bounds; the support-and-norm constants (13) can be used without numerically sampling the functions.

4) **Certify the full wavelet bases when needed.** Use the cross-filters to refine the two wavelets. Check the transformed mask zeros and Fourier decay (17); the seed condition $C_c^{s+1+\delta}$ is one sufficient way to obtain that decay. Theorem 4.3 then gives dual Riesz bases across all dyadic scales. Without this last check, Steps 1-3 certify the scaling functions and their single-scale translate bounds, but not global stability.

The *D*8 and *D*24 examples execute these steps using precisely defined initial filters. Section 7 certifies a new rational *choice of coefficients* within a known spline mask family and then executes the same procedure; no general novelty is attributed to the transfer operation itself.

4.2. A Reusable Certification Procedure

The construction above separates algebraic filter operations from functional admissibility. The following procedure makes the bounds and finite certificates reproducible for other specified filters. Rational arithmetic is used when the mask coefficients are rational; for other coefficients one needs rigorous enclosures or independent analytic bounds.

1) **Check the algebraic input.** Verify normalization, the alias identity, the support indices and the zero orders at −1. For an order-s transfer, perform exact

Laurent division by A^s on the dual side. These tests alone do not establish L^2 existence.

2) **Certify the required regularity.** Use a known regularity theorem, or factor a normalized mask as A^pQ. For an integer $q \geq 1$, obtain a certified bound

$$\sup_{\omega} \prod_{r=0}^{q-1} \left| Q\left(\mathrm{e}^{-\mathrm{i}2^r\omega}\right) \right| \leq M_q, \quad M_q \geq 1.$$

Grouping the refinement product into blocks of q factors, with its small-argument tail bounded using $Q(1)=1$, gives Fourier decay with exponent $\alpha = p - q^{-1}\log_2 M_q$. The strict inequality $\alpha > s + 1/2$ ensures H^s regularity and decay above 1/2 after an inverse transfer of order s, by canceling the s box factors in the factorized product. Check the primal decay separately. When $Q\left(\mathrm{e}^{-\mathrm{i}\omega}\right) = R\left(\sin^2(\omega/2)\right)$, partition $[0,1]$ into rational intervals, enclose their images under $y \mapsto 4y(1-y)$, and use the largest absolute Bernstein coefficient on each interval. For $q=2$, the products of these interval bounds give M_2 as in (47). If instead $|Q|^2 = P$, bound the products of P and take the square root, as in Proposition 5.1.

3) **Certify biorthogonality.** Once the normalized compact L^2 functions exist, form the cross-correlation recurrence on the finite index range fixed by their supports. Prove that its nullspace is one-dimensional and that its normalization selects δ_0. A nonzero integer minor modulo a prime provides an exact rank witness; justify the normalization using a partition of unity.

4) **Compute the translate bounds.** If only supports and certified upper bounds for $\|\phi\|_2$ and $\left\|\tilde{\phi}^{(s)}\right\|_2$ are available, insert them in (13). For sharper bounds, solve each autocorrelation recurrence separately and prove uniqueness after normalization. Its exact solution gives $B(f) = \sum_m \left|\left\langle f, f(\cdot - m)\right\rangle\right|$; apply (12). A cross-correlation rank witness does not replace either autocorrelation uniqueness check.

5) **Record the conclusion and its limits.** For full wavelet bases, verify the remaining mask zeros and apply Theorem 4.3. Record the rational interval partition, strict comparisons, index ranges and rank witnesses so that the certificate can be rerun. Failure of a sufficient bound is inconclusive: refine the enclosure or use another criterion before making an existence claim.

The geometric bounds require the indicated norm bounds as inputs; they do not compute derivative norms from support length alone. The exact examples below use the same procedure with different regularity and correlation certificates.

5. Admissible Examples

5.1. An Exact Spline Pair

Let $B_m = b^{*m}$. A known CDF spline pair [2] has B_2 on the dual side and masks

$$\tilde{H}(z) = A(z)^2, \quad H(z) = A(z)^2\left(2 - \frac{z+z^{-1}}{2}\right). \tag{19}$$

The cited construction provides the compact L^2 seed and its functional biorthogonality. In this instance $B_2 \in H^1$ and, exactly,

$$\left(T^*\right)^{-1} B_2 = b(\cdot - 1) = \mathbf{1}_{[1,2]}, \quad T^* \mathbf{1}_{[1,2]} = B_2. \tag{20}$$

The dual translates are orthonormal, so $B\left(\tilde{\Phi}_1\right) = 1$ and the lower primal translate Riesz constant is 1. The transformed masks are $H_1(z) = A(z)^3 \left(2 - \left(z + z^{-1}\right)/2\right)$ and $\tilde{H}_1(z) = zA(z)$. Table 2 gives *all four* resulting refinement and cross-filter sequences in the convention $H_1(z) = \frac{1}{2}\sum h_k^{(1)} z^k$.

Table 2. Exact taps for the B_2 seed after one factor transfer; zero taps are displayed explicitly.

k	$h_k^{(1)}$	$\tilde{h}_k^{(1)}$	g_k	$\tilde{g}_k$
−3	0	0	0	1/8
−2	0	0	0	1/8
−1	−1/8	0	−1	−1
0	1/8	0	1	1
1	1	1	0	−1/8
2	1	1	0	−1/8
3	1/8	0	0	0
4	−1/8	0	0	0

This example also has *exact numerical Riesz constants*. The primal scaling function Φ_1 has support in $[-1,4]$. For $c_m = \langle \Phi_1, \Phi_1(\cdot - m) \rangle$, its refinement equation and partition of unity give the finite system

$$\begin{aligned} c_m &= \frac{1}{2}\sum_{i,j} h_i^{(1)} h_j^{(1)} c_{2m+j-i}, \\ c_{-m} &= c_m, \quad c_m = 0 \left(|m| \geq 5\right), \\ \sum_m c_m &= 1. \end{aligned}$$

The homogeneous recurrence on indices $-4, \cdots, 4$ has rank eight; adjoining $\sum_m c_m = 1$ gives rank nine. Thus, the normalized system determines the actual correlations uniquely. Exact rational elimination yields $c_0 = 13/12$, $c_1 = -1/36$, $c_2 = -1/72$ and $c_m = 0$ for $3 \leq m \leq 4$; substitution verifies every recurrence equation and the normalization. The Gram symbol therefore is

$$G(\theta) = \frac{13}{12} - \frac{\cos\theta}{18} - \frac{\cos(2\theta)}{36} = \frac{9}{8} - \frac{(\cos\theta + 1/2)^2}{18}, \quad 1 \leq G(\theta) \leq \frac{9}{8}.$$

Both extrema are attained. Thus, for every finitely supported $a = (a_k)$,

$$\|a\|_{\ell^2}^2 \leq \left\| \sum_k a_k \Phi_1(\cdot - k) \right\|_2^2 \leq \frac{9}{8} \|a\|_{\ell^2}^2, \quad \left\| \sum_k a_k \tilde{\Phi}_1(\cdot - k) \right\|_2^2 = \|a\|_{\ell^2}^2. \tag{21}$$

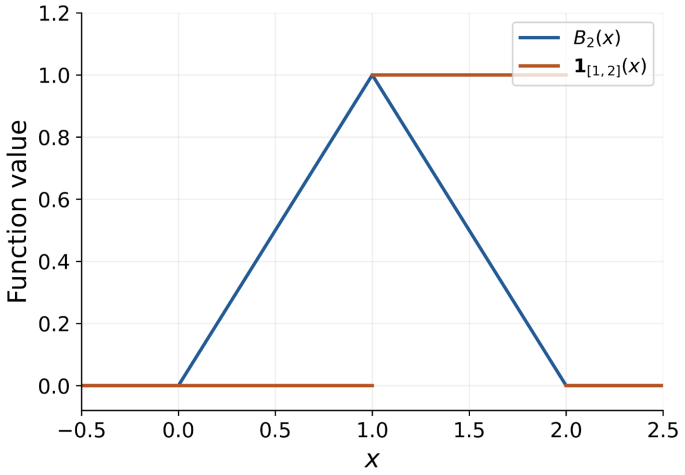

Figure 1. Exact spline inverse $B_2 = T^* \mathbf{1}_{[1,2]}$. The orange segments show its discontinuous inverse.

Figure 1 displays B_2 and its exact inverse (20). More generally,

$$\left(T^*\right)^{-s} B_m = B_{m-s}\left(\cdot - s\right), \quad 1 \le s < m. \tag{22}$$

For $m = 4$, the inverses at $s = 1,2$ are $B_3\left(\cdot - 1\right)$ and $B_2\left(\cdot - 2\right)$. This certifies the spline inverse, not the other member of any proposed 4/4 pair.

5.2. Daubechies with Four Vanishing Moments

Let ϕ_D be the normalized orthonormal Daubechies scaling function with four wavelet vanishing moments (the eight-tap $D8$ filter, or db4). Choose standard support $\left[0,7\right]$ and take $\tilde{\phi} = \phi = \phi_D$. Daubechies [11] establishes compact support, orthonormal translates and an order-four mask zero at -1. The wavelet exponent $1.61792\cdots$ reported in ([12], Table 6), together with Lemma 4.4, gives $\phi_D \in C_c^{1,1/2}\left(\mathbb{R}\right) \subset H^1\left(\mathbb{R}\right)$. Corollary 2 applies and gives

$$\Phi_D = b * \phi_D, \quad \tilde{\Phi}_D\left(x\right) = \sum_{k=1}^{\infty} \phi_D'\left(x - k\right). \tag{23}$$

At most seven terms contribute; its support lies in $\left[1,7\right]$. Its finite masks are $H_D A$ and $H_D z / A$, with respective zero orders five and three at -1. Functional biorthogonality follows from Theorem 3.1. The orthonormal seed and L^2 contraction of T give an upper translate Riesz constant of 1 for Φ_D. The inverse estimate gives $\left\|\tilde{\Phi}_D\right\|_2 \le 7\left\|\phi_D'\right\|_2$; at most 13 correlation shifts meet its support, so $B\left(\tilde{\Phi}_D\right) \le 637\left\|\phi_D'\right\|_2^2$. Explicit squared-norm Riesz bounds are therefore

$$\frac{\|c\|_{\ell^2}^2}{637\left\|\phi_D'\right\|_2^2} \le \left\|\sum_k c_k \Phi_D\left(\cdot - k\right)\right\|_2^2 \le \|c\|_{\ell^2}^2, \tag{24}$$

$$\|c\|_{\ell^2}^2 \le \left\|\sum_k c_k \tilde{\Phi}_D\left(\cdot - k\right)\right\|_2^2 \le 637\left\|\phi_D'\right\|_2^2 \|c\|_{\ell^2}^2.$$

These conservative constants are finite and certified. **Figure 2** illustrates the

three functions with the transformed *finite masks*, not a difference quotient of sampled scaling functions. The cascade was run for 12 levels and plotted as dyadic cell averages at level 9; the L^2 difference between the level-11 and level-12 averaged dual displays is about 2.93×10^{-3}. Its small-scale roughness is consistent with limited regularity; the picture is not a proof of the existence or stability claims.

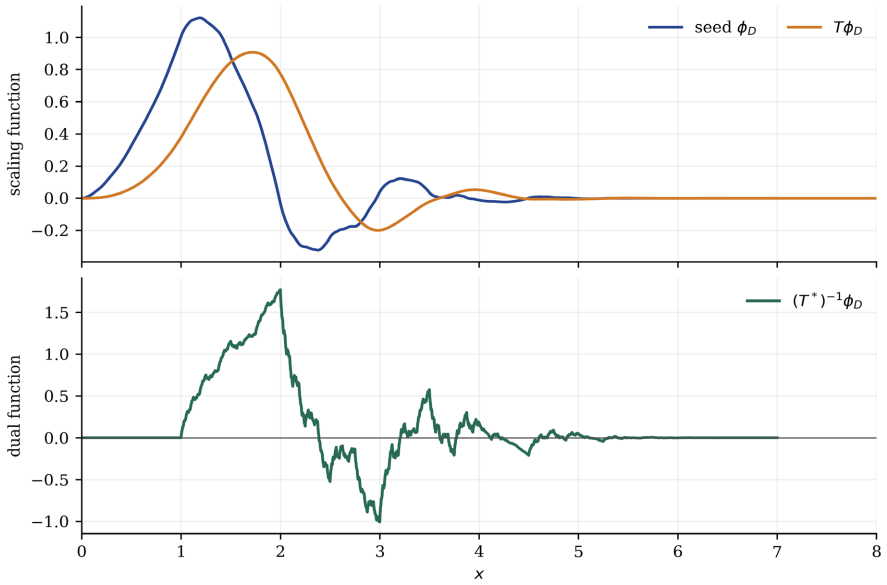

Figure 2. The *D*8 seed and its transformed scaling partners. Direct mask cascades (12 levels), plotted with level-9 dyadic cell averages; no numerical differentiation is used. The exact filter relations, not the plot, support the analysis.

This is one concrete application of the 2009 construction [1]. The original **Figure 3** [1] omits the exact tap ordering and phase, so we do not identify this canonical example with every detail of that illustration. He [7] already studied transfers of Daubechies seeds; no new family is claimed here. The published Hölder exponent is strictly larger than 1.55: choosing $\delta = 0.55$ and using Lemma 4.4 gives $\phi_D \in C_c^{1,.55}$. The finite inverse sum (23) then gives $\tilde{\Phi}_D \in C_c^{0,.55}$, and box convolution gives $\Phi_D \in C_c^{2,.55}$. Integration by parts and a finite-difference estimate imply Fourier decay exponents 0.55 and 2.55, respectively. Both exceed the 1/2 threshold in Theorem 4.3; the two transferred masks have the required zeros. Thus, the *D*8 cross-filter wavelets also form dual Riesz bases across all scales. These global bounds are positive and finite, although (24) only quantifies the simpler translate bounds.

5.3. Two Full-Scale Examples from a 24-Tap Seed

There is an explicit high-regularity seed for which the cross-scale conclusion is also available. Let ϕ_{12} be the standard real, minimum-phase Daubechies scaling function with twelve vanishing moments, normalized by $\int \phi_{12} = 1$ and $\operatorname{supp}\phi_{12} \subset [0,23]$. Its 24-tap mask $H_{12}(z) = \frac{1}{2}\sum_{k=0}^{23} h_k z^k$ is specified uniquely by

the minimum-phase spectral factorization, $H_{12}(1)=1$, and

$$\begin{aligned} &\left|H_{12}\left(\mathrm{e}^{-\mathrm{i}\omega}\right)\right|^2=(1-y)^{12}P_{11}(y),\\ &y=\sin^2(\omega/2),\\ &P_{11}(y)=\sum_{r=0}^{11}\binom{11+r}{r}y^r. \end{aligned} \tag{25}$$

These exact algebraic conditions determine the finite filter without rounding its taps. The original construction [11] proves that ϕ_{12} is compactly supported with orthonormal integer translates and that its mask has a zero of order twelve at −1. Guglielmi and Protasov ([12], Section 6 and Table 6) compute the Hölder exponent $3.83348\cdots$ of the *wavelet* ψ_{12}. For the strict exponent 3 + 1/2 this means $\psi_{12}\in C_c^{3,1/2}(\mathbb{R})$; Lemma 4.4 then proves, separately, $\phi_{12}\in C_c^{3,1/2}(\mathbb{R})$. This passage from wavelet to scaling regularity is required for the application of Theorem 4.3 below.

For each $s\in\{1,2\}$ set

$$\Phi_{12,s}=b^{*s}*\phi_{12},\quad \tilde{\Phi}_{12,s}(x)=\sum_{k=s}^{\infty}\binom{k-1}{s-1}\phi_{12}^{(s)}(x-k). \tag{26}$$

The sum is finite pointwise, supported in $[s,23]$. Both functions lie in L^2; they are biorthogonal under integer translation. Their finite refinement masks are

$$H_{12,s}(z)=H_{12}(z)A(z)^s,\quad \tilde{H}_{12,s}(z)=H_{12}(z)\left(z/A(z)\right)^s. \tag{27}$$

They have zero orders $12+s$ and $12-s$ at −1.

Proposition 5.1 (exact two-level decay). For the mask (25), set $P=P_{11}$, $a_i=i/32$, $b_i=(i+1)/32$, and

$$M_i=\begin{cases}1, & a_i\le 1/2\le b_i,\\ \max\left\{4a_i(1-a_i),4b_i(1-b_i)\right\}, & \text{otherwise.}\end{cases}$$

The exact rational inequalities

$$\max_{0\le i<32}P(b_i)P(M_i)<2^{34} \tag{28}$$

hold. Consequently, for a constant independent of ξ,

$$\left|\hat{\Phi}_{12,s}(\xi)\right|\le C_s\left(1+|\xi|\right)^{-7/2-s},\quad \left|\hat{\tilde{\Phi}}_{12,s}(\xi)\right|\le C_s\left(1+|\xi|\right)^{-7/2+s},\quad s=1,2. \tag{29}$$

In particular, the seed is in H^2 and (17) holds for both transfers with $\varepsilon=1/2$.

Proof. We use the two-factor certification procedure of Section 4.2, here with $|Q_{11}|^2=P$. The polynomial P is increasing on $[0,1]$. On the ith interval, $y\le b_i$ and $4y(1-y)\le M_i$; this reduces the continuous inequality $P(y)P(4y(1-y))<2^{34}$ to the 32 rational comparisons (28). Their largest left-hand side occurs at $i=21$ and is less than 2^{34} by integer cross multiplication. The companion exact certificate script performs all 32 comparisons with rational numbers.

Write $H_{12}=A^{12}Q_{11}$. Since $\left|Q_{11}\left(\mathrm{e}^{-\mathrm{i}\omega}\right)\right|^2=P\left(\sin^2(\omega/2)\right)$, the double-angle

identity and (28) give

$$\left|Q_{11}\left(\mathrm{e}^{-\mathrm{i}\omega}\right)Q_{11}\left(\mathrm{e}^{-2\mathrm{i}\omega}\right)\right|<2^{17}.$$

Grouping the factors two by two in the Fourier product for ϕ_{12}, and bounding the small-argument tail using $Q_{11}(1)=1$, yields

$$\hat{\phi}_{12}(\xi)=\tau(\xi)^{12}\prod_{j\geq 1}Q_{11}\left(\mathrm{e}^{-\mathrm{i}\xi/2^{j}}\right),\quad \prod_{j\geq 1}\left|Q_{11}\left(\mathrm{e}^{-\mathrm{i}\xi/2^{j}}\right)\right|\leq C\left(1+|\xi|\right)^{17/2}.$$

As $|\tau(\xi)|\leq\min\{1,2/|\xi|\}$ and $|\tau/\tau_{-}|=1$ away from the removable zeros, the multipliers of (2) imply (29). The seed estimate with $s=0$ is $O\left(\left(1+|\xi|\right)^{-7/2}\right)$, which implies H^{2} by Plancherel. □

The factor $H_{12}=A^{12}Q_{11}$, with Q_{11} an eleven-degree polynomial, gives the exact tap ranges and vanishing-moment counts in Table 3. The $D8$ row records the preceding example; the rational spline-seed example below is listed separately.

Table 3. Support of the low-pass tap sequences, mask zero orders at −1, and vanishing moments of $\left(\Psi_{s},\tilde{\Psi}_{s}\right)$.

Seed, s	$k:\left(h^{(s)},\tilde{h}^{(s)}\right)$	$\mathrm{ord}_{-1}\left(H_{s},\tilde{H}_{s}\right)$	moments $\left(\Psi_{s},\tilde{\Psi}_{s}\right)$
$D8,1$	$(0:8,1:7)$	$(5,3)$	$(3,5)$
$D24,1$	$(0:24,1:23)$	$(13,11)$	$(11,13)$
$D24,2$	$(0:25,2:23)$	$(14,10)$	$(10,14)$

Figure 3 shows the two frequency responses; these curves are determined by the exact spectral factorization (25) and are *mask moduli*, not additional claims about the historical scaling functions.

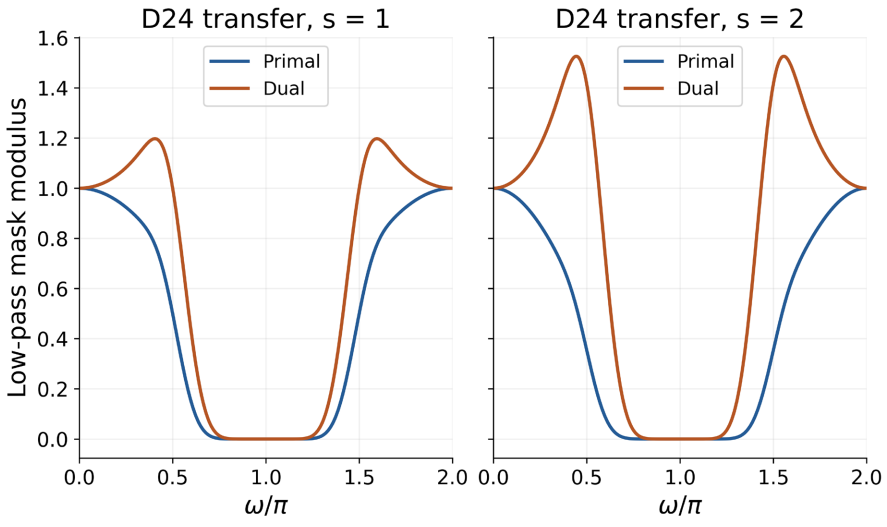

Figure 3. Exact moduli of the $D24$ transformed low-pass masks for $s=1,2$. The increasing difference between the two masks expresses the transfer of a spline factor; both vanish at $\omega=\pi$.

The bounds from Theorem 3.1 can be sharpened on the primal side because ϕ_{12} has orthonormal translates and convolution by b^{*s} is an L^2 contraction. Put

$$C_{12,s} = \left(2(23-s)+1\right)\binom{23}{s}^2 \left\|\phi_{12}^{(s)}\right\|_2^2. \tag{30}$$

For every finitely supported c, the explicit translate bounds are

$$C_{12,s}^{-1}\|c\|_{\ell^2}^2 \le \left\|\sum_k c_k \Phi_{12,s}(\cdot - k)\right\|_2^2 \le \|c\|_{\ell^2}^2, \tag{31}$$

$$\|c\|_{\ell^2}^2 \le \left\|\sum_k c_k \tilde{\Phi}_{12,s}(\cdot - k)\right\|_2^2 \le C_{12,s}\|c\|_{\ell^2}^2.$$

In particular $C_{12,1} = 23805\|\phi_{12}'\|_2^2$ and $C_{12,2} = 2752387\|\phi_{12}''\|_2^2$. These are explicit positive finite constants defined by the exact filter (25).

Theorem 4.3 applies for $s=1$ and $s=2$ with $\varepsilon = 1/2$ by Proposition 5.1, and both masks retain sum rules. Independently, the published wavelet regularity and Lemma 4.4 also give the smooth-seed sufficient condition. Thus the two cross-filter systems for each value of s form *dual Riesz bases of* $L^2(\mathbb{R})$ *across all scales*, with positive finite global constants as in (18). The two values of s yield fully specified functional scaling pairs and wavelet bases constructed by the procedure of Section 4.1.

6. Degree-Minimal Symmetric Spline Duals: An Obstruction

This section tests the essential *input certification* in Step 1 of Section 4.1. The algebraic spline complement in this class is familiar from CDF's B-spline construction ([2], Section 6.A); the 4/4 lack of L^2 regularity was subsequently reported [10]. We specify its precise mask constraints and prove an all-orders L^2 obstruction. The result is restricted to this class; it makes no assertion that all higher-order biorthogonal spline pairs fail to exist.

Theorem 6.1 (obstruction from order four onward). For an integer $m \ge 1$ put $H_{B,m}(z) = A(z)^m$ and $y(z) = \left(2 - z - z^{-1}\right)/4$. Suppose that a real Laurent mask $H_{C,m}$ is symmetric about $m/2$ (that is, $H_{C,m}(z) = z^m H_{C,m}(z^{-1})$), supported in the exponent range $[-m+1, 2m-1]$, has a zero of order at least m at -1, and satisfies

$$H_{B,m}(z)H_{C,m}(z^{-1}) + H_{B,m}(-z)H_{C,m}(-z^{-1}) = 1. \tag{32}$$

Then there is exactly one such mask:

$$H_{C,m}(z) = A(z)^m P_{m-1}(y(z)), \quad P_{m-1}(y) = \sum_{r=0}^{m-1}\binom{m-1+r}{r} y^r. \tag{33}$$

For every $m \ge 4$, there is *no* compactly supported $L^2(\mathbb{R})$ function u with $\int u = 1$ refined by this mask. Consequently, (32) does not define a compact L^2 biorthogonal scaling pair for any of these orders.

Proof. Divisibility at -1 and the support constraint write $H_{C,m} = A^m Q(z)$, where Q is a Laurent polynomial with exponents between $-m+1$ and $m-1$. The stated symmetry and $A(z)^m = z^m A\left(z^{-1}\right)^m$ imply $Q(z) = Q\left(z^{-1}\right)$. Hence Q is a polynomial of degree at most $m-1$ in $z+z^{-1}$, equivalently in $y(z)$. On the unit circle, (32) becomes

$$(1-y)^m Q(y) + y^m Q(1-y) = 1. \tag{34}$$

Reducing modulo y^m shows that Q is the degree-$(m-1)$ Taylor polynomial of $(1-y)^{-m}$, namely P_{m-1}. Conversely, the polynomial $1-(1-y)^m P_{m-1}(y) - y^m P_{m-1}(1-y)$ is divisible by both y^m and $(1-y)^m$ and has degree at most $2m-1$, so it is identically zero. This also proves uniqueness in the stated class.

At the two points $2\pi/3$ and $4\pi/3$, doubling modulo 2π swaps the points, $y = 3/4$, and the mask modulus is

$$q_m = 2^{-m} P_{m-1}(3/4). \tag{35}$$

Exact arithmetic gives $q_4 = 289/256$, $q_5 = 6413/4096$, and $q_6 = 35995/16384$, all greater than 1. For $m \geq 7$, the last positive summand of (35) alone is

$$L_m = 2^{-m}\binom{2m-2}{m-1}(3/4)^{m-1},$$

$$L_7 = 168399/131072 > 1,$$

$$\frac{L_{m+1}}{L_m} = \frac{3(2m-1)}{4m} > 1.$$

Thus $q_m > 1$ for all $m \geq 4$.

If u as in the statement existed, compact support and $u \in L^2$ would imply $u \in L^1$ and $\hat{u}$ bounded and continuous with $\hat{u}(0) = 1$. Iterating refinement backwards from $t_0 = 2\pi/3$ yields $\hat{u}(t_0) = \prod_{j\geq 1} H_{C,m}\left(\mathrm{e}^{-\mathrm{i}t_0/2^j}\right) \neq 0$: each factor is nonzero because $P_{m-1}(y) > 0$ for $0 \leq y < 1$, and the factors approach 1 at a summable rate. Forward refinement on the doubling cycle gives $\left|\hat{u}\left(2^j t_0\right)\right| = q_m^j \left|\hat{u}(t_0)\right|$, contrary to boundedness. The same argument also rules out compactly supported normalized L^1 refinable functions. □

6.1. The Rational Order-Four Case

The case $m = 4$ gives one fully explicit counterexample to inferring scaling functions from a perfect-reconstruction identity. Set

$$\begin{aligned} y(z) &= \frac{2 - z - z^{-1}}{4}, \\ P_3(y) &= 1 + 4y + 10y^2 + 20y^3, \\ H_B(z) &= A(z)^4, \\ H_C(z) &= A(z)^4 P_3(y(z)). \end{aligned} \tag{36}$$

For $|z|=1$, put $y=\sin^2(\arg z/2)$. The masks are explicit Laurent polynomials: $H_B=\sum_k b_k z^k$ and $H_C=\sum_k c_k z^k$, with the exact coefficients in Table 4. Our refinement convention is $u(x)=2\sum_k c_k u(2x-k)$, so the refinement taps are $2c_k$. The coefficients b_k for $k=0,\cdots,4$ are $(1,4,6,4,1)/16$.

Table 4. Exact coefficients of the counterexample mask H_C; values are shown as $256c_k$.

k	$256c_k$	k	$256c_k$
−3	−5	3	70
−2	20	4	−96
−1	−1	5	−1
0	−96	6	20
1	70	7	−5
2	280		

These two finite masks satisfy the algebraic identity

$$(1-y)^4 P_3(y)+y^4 P_3(1-y)=1 \tag{37}$$

for every real y: it follows by expanding the two degree-seven polynomials. On the unit circle this is exactly $H_B(z)\overline{H_C(z)}+H_B(-z)\overline{H_C(-z)}=1$. The first mask refines the cubic spline $B_4\in L^2$.

Proposition 6.2 (rational 4/4 obstruction). There is no compactly supported $u\in L^2(\mathbb{R})$ with $\int u=1$ satisfying $u(x)=2\sum_{k=-3}^{7} c_k u(2x-k)$, where c_k are exactly those in Table 4. In particular, these perfect-reconstruction masks cannot define a compactly supported L^2 biorthogonal scaling pair.

Proof. This is Theorem 6.1 at $m=4$. For clarity, the cycle argument also yields a direct L^2 contradiction without relying on a pointwise L^∞ bound: Set $t_0=2\pi/3$. Its doubling orbit modulo 2π alternates between $2\pi/3$ and $4\pi/3$, where $y=3/4$. At both angles the mask modulus equals

$$q=\frac{1}{16}P_3(3/4)=\frac{289}{256}>1. \tag{38}$$

If u existed, $\hat{u}$ would be continuous with $\hat{u}(0)=1$. Iterating refinement at t_0 gives $\hat{u}(t_0)=\prod_{j\geq 1} H_C\left(\mathrm{e}^{-\mathrm{i}t_0/2^j}\right)\neq 0$: all factors are nonzero and converge sufficiently quickly to 1. For $\xi_j=2^j t_0$, refinement gives $\left|\hat{u}(\xi_j)\right|=q^j\left|\hat{u}(t_0)\right|$.

For a general Fourier L^2 function, pointwise growth alone is insufficient. Fix small $\varepsilon>0$, $|v|\leq\varepsilon$, and iterate at ξ_j+v. The initial factor $\hat{u}(t_0+v/2^j)$ stays away from zero. The other factors lie within $\varepsilon/2^{j-r}$ of the two nonzero orbit values. Since $\log\left|H_C\left(\mathrm{e}^{-\mathrm{i}t}\right)\right|$ is Lipschitz near those values and $\sum_{r=0}^{j-1}2^{-(j-r)}<1$, their product is at least Cq^j for a constant $C>0$ independent of j,v. The fixed-width intervals $[\xi_j-\varepsilon,\xi_j+\varepsilon]$ are eventually disjoint and each has Fou-

rier L^2 mass at least $2\varepsilon C^2 q^{2j}$, a contradiction. □

Figure 4 displays the two marked orbit values used in Proposition 6.2. Figure 5 places this order-four example in the family of Theorem 6.1 by plotting the exact values q_m.

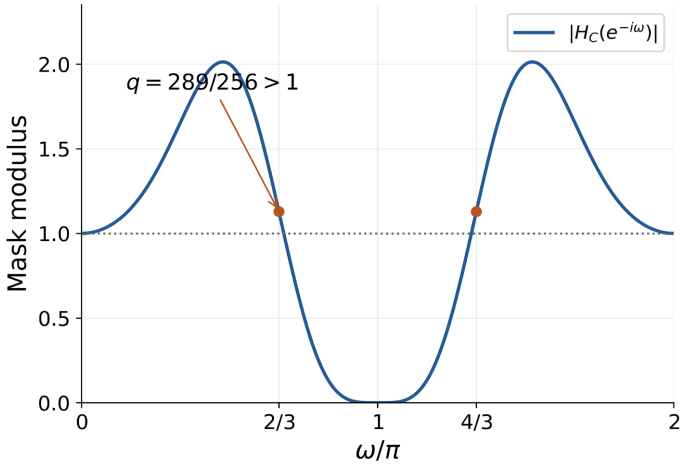

Figure 4. Mask modulus of the rational counterexample. Doubling alternates between $2\pi/3$ and $4\pi/3$; the modulus equals $q = 289/256 > 1$ at both points. The proof uses positive-width frequency intervals, not only the marked points.

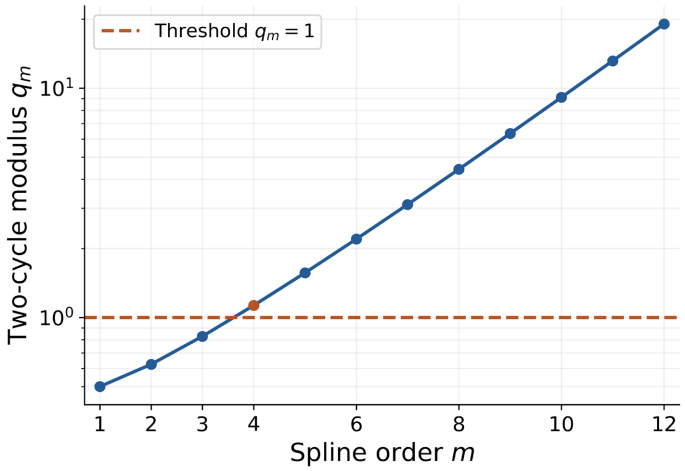

Figure 5. The exact two-cycle modulus q_m from (35). The crossing at $m = 4$ proves the obstruction for orders $4,5,6$; the last-term inequality in the proof covers all $m \geq 7$. Points are plotted from rational values.

6.2. The Historical 4/4 Illustrations

The notation "B-spline 4 4" in the 2009 [1] figure captions does not specify a unique seed filter. To see this at the algebraic level, the masks above belong to a family of possible finite perfect-reconstruction filters. For any real polynomial S let

$$Q_S(y) = P_3(y) + y^4(1-2y)S\big(y(1-y)\big), \quad H_{C,S}(z) = A(z)^4 Q_S\big(y(z)\big). \tag{39}$$

In fact, the extra contribution to the left-hand side of (37) is $(1-y)^4 y^4\left[(1-2y)+(1-2(1-y))\right]S(y(1-y))=0$. Thus, every choice of S gives a normalized symmetric real *perfect-reconstruction filter partner* for H_B; different choices already have different taps. This is an algebraic nonuniqueness statement, not an existence claim for L^2 scaling functions: $S=0$ is ruled out by Proposition 6.2. It limits only retrospective identification of the particular plotted curves. The forward construction of Section 4.1 takes a specified admissible seed and does not require the coefficients of those illustrations. Even with the plotted taps, one would still need the L^2 and stability checks for their particular seed. For example, applying (15) *formally* to the counterexample $S=0$ gives the fully calculable filters

$$H_{B,s}(z)=A(z)^{4+s},\quad H_{C,s}(z)=z^s A(z)^{4-s}P_3(y(z)),\quad s=1,2. \tag{40}$$

They remain algebraic perfect-reconstruction filters; the obstruction in Proposition 6.2 prevents their interpretation as transfers of a valid compact L^2 seed pair.

7. A Rational Spline Seed and Transfer

The Daubechies transfers start from established orthonormal seeds. We now specify a nonorthogonal seed by *rational* coefficients, certify that it is an actual biorthogonal scaling pair, and execute the 2009 [1] transfer on it. This choice belongs to the free Bézout family of CDF [2]; the claim here is the particular coefficient choice and its exact functional certificate, not the invention of spline-based biorthogonal wavelets. Put $A(z)=(1+z)/2$, $y(z)=\left(2-z-z^{-1}\right)/4$, and

$$\begin{aligned} P_3(y)&=1+4y+10y^2+20y^3,\\ R(y)&=P_3(y)+y^4(2y-1)\{-32-280y(1-y)\}\\ &=1+4y+10y^2+20y^3+32y^4+216y^5-840y^6+560y^7. \end{aligned} \tag{41}$$

This is the choice $S(u)=32+280u$ in (39); the degree-minimal case is $S=0$. To explain the design criterion, restrict that free family to the affine corrections $S(u)=a+bu$. Perfect reconstruction then holds identically for every (a,b), while the degree of R is at most seven and the dual mask occupies at most the 19 positions $-7:11$. The analytic target for one inverse transfer is a two-factor bound

$$\sup_{0\le y\le 1}\left|R(y)R(4y(1-y))\right|<32.$$

By the procedure of Section 4.2, this gives $\alpha=4-\frac{1}{2}\log_2 M>3/2$: the seed dual belongs to H^1, and the transferred dual has Fourier decay exponent $\alpha-1>1/2$. The rational point $(a,b)=(32,280)$ meets this target, as certified below, with a finite filter of manageable length. It is presented as an explicit admissible example within this two-parameter family. We claim neither optimal regularity or Riesz bounds nor a shortest possible support; no global optimization or exhaustive

search is asserted.

Theorem 7.1 (Rational order-four seed and its transfer). The normalized finite masks

$$H_0(z)=A(z)^4,\quad \tilde{H}_0(z)=A(z)^4R\big(y(z)\big) \tag{42}$$

refine a compactly supported biorthogonal L^2 pair $\left(B_4,\tilde{\phi}_0\right)$, with $\operatorname{supp}\tilde{\phi}_0\subset[-7,11]$ and $\tilde{\phi}_0\in H^1(\mathbb{R})$. The one-step transfer

$$\Phi_1=TB_4=B_5,\quad \tilde{\Phi}_1=\left(T^*\right)^{-1}\tilde{\phi}_0 \tag{43}$$

is a compactly supported biorthogonal scaling pair with masks

$$H_1(z)=A(z)^5,\quad \tilde{H}_1(z)=zA(z)^3R\big(y(z)\big). \tag{44}$$

The seed dual has 19 nonzero tap positions $-7:11$; the transferred dual has 18 positions $-6:11$. For every finitely supported sequence c,

$$\frac{1}{48}\|c\|_{\ell^2}^2\le\left\|\sum_k c_k\Phi_1(\cdot-k)\right\|_2^2\le\|c\|_{\ell^2}^2, \tag{45}$$

$$\|c\|_{\ell^2}^2\le\left\|\sum_k c_k\tilde{\Phi}_1(\cdot-k)\right\|_2^2\le 48\|c\|_{\ell^2}^2.$$

Their cross-filter wavelets are dual Riesz bases of $L^2(\mathbb{R})$ across all dyadic scales; the primal and dual wavelets have, respectively, three and five vanishing moments.

Proof. The Bézout identity $(1-y)^4P_3(y)+y^4P_3(1-y)=1$ is exact. The correction in (41) is antisymmetric under $y\mapsto 1-y$, so $(1-y)^4R(y)+y^4R(1-y)=1$. This is the exact low-pass alias identity for (42); multiplication by A and z/A also gives it for (44). All four masks equal one at $z=1$. The Laurent support of $R\big(y(z)\big)$ is $[-7,7]$, giving the asserted seed and transferred tap intervals.

It remains to establish that the seed dual is a *function*. The normalized infinite refinement product for $\tilde{H}_0$ defines a compactly supported distribution: the finite Laurent mask and its value 1 at $z=1$ give the entire product with polynomial growth and finite exponential type, as in CDF ([2], Lemma 3.1). Directly, separate the product at $J=\left\lceil\log_2\left(1+|\zeta|\right)\right\rceil$; the first J Laurent factors have polynomial growth times $\mathrm{e}^{7|\operatorname{Im}\zeta|}$, and the remaining product is uniformly bounded because $R(0)=1$. The infinite product of the A^4 factors is $\tau(\zeta)^4=\hat{B}_4(\zeta)$, whose inverse Fourier transform has support $[0,4]$. The Laurent R product contributes $[-7,7]$, giving $[-7,11]$ for the dual distribution. On the real axis, with τ from (3),

$$\widehat{\tilde{\phi}_0}(\xi)=\tau(\xi)^4\prod_{j\ge 1}R\left(\sin^2\frac{\xi}{2^{j+1}}\right). \tag{46}$$

For $I_i=\left[i/64,(i+1)/64\right]$, let J_i be the smallest interval containing $\{4y(1-y):y\in I_i\}$. Denote by $\beta(F,I)$ the largest absolute Bernstein coeffi-

cient of the polynomial F after affine substitution from I to $[0,1]$. The Bernstein convex-hull bound and *exact rational* arithmetic give the finite certificate

$$\max_{0\le i<64}\beta(R,I_i)\beta(R,J_i)=\frac{218570696039581571133220 3}{75557863725914323419136}<32. \tag{47}$$

The maximum occurs at $i=48$. The Python script available from the author upon request computes all 64 Bernstein enclosures using exact rational arithmetic. Since consecutive dyadic arguments in (46) are related by $y\mapsto 4y(1-y)$, pair the factors, and bound the small-argument tail using $R(0)=1$. Thus

$$\left|\widehat{\tilde{\phi}_0}(\xi)\right|\le C(1+|\xi|)^{-\alpha},\quad \alpha=4-\frac{1}{2}\log_2 M>\frac{3}{2}, \tag{48}$$

where M is the rational number in (47). Plancherel proves $\tilde{\phi}_0\in L^2\cap H^1$; $B_4\in H^1$ as well.

For clarity, we also certify *functional* biorthogonality instead of inferring it from the filter identity. Let $c_m=\langle B_4,\tilde{\phi}_0(\cdot-m)\rangle$. The supports give $c_m=0$ for $|m|\ge 11$. With the tap convention $H=\frac{1}{2}\sum h_i z^i$, refinement gives

$$c_m=\frac{1}{2}\sum_{i,j}h_i\tilde{h}_j c_{2m+j-i},\quad -10\le m\le 10. \tag{49}$$

The 21×21 rational matrix $I-\mathcal{T}$ of (49) has rank 20: its column for $m=0$ vanishes by the alias identity, and deleting that column and its row, then multiplying the resulting 20×20 matrix by 2^{17}, gives an integer determinant equal to 2 modulo 101. Hence its nullspace is spanned by δ_0. The B_4 translates partition unity and $\int\tilde{\phi}_0=1$ by normalization; consequently $\sum_m c_m=1$ and $c_m=\delta_{m0}$.

For the two dual functions, the autocorrelation calculations require separate uniqueness certificates. For either $f=\tilde{\phi}_0$ or $f=\tilde{\Phi}_1$, refinement, the mask zero at −1, and normalization imply $\hat{f}(2\pi n)=\delta_{n0}$ for every integer n. Indeed, at a nonzero integer frequency, iterating refinement reaches an odd multiple of π in a mask factor. The periodization $P_f(t)=\sum_{k\in\mathbb{Z}}f(t+k)$ belongs to $L^2(0,1)$ by compact support, and its Fourier coefficients are $\hat{f}(2\pi n)$. Hence $P_f=1$ almost everywhere, which gives

$$\sum_m r_m=\int_0^1|P_f(t)|^2\,\mathrm{d}t=1,\quad r_m=\langle f,f(\cdot-m)\rangle.$$

The transferred function exists by Theorem 2.3 and Corollary 4.2, since the seed dual is in H^1 and its mask has a fourth-order zero at −1.

Let h^f denote the refinement taps of f. On $\mathcal{I}_n=\{-n,\cdots,n\}$ define

$$(C_f r)_m=r_m-\frac{1}{2}\sum_{i,j}h_i^f h_j^f r_{2m+j-i},\quad r_k=0\ \ (k\notin\mathcal{I}_n). \tag{50}$$

The support intervals give $n=17$ for $\tilde{\phi}_0$ and $n=16$ for $\tilde{\Phi}_1$; endpoint-only overlaps have zero integral. Form D_f by replacing the row $m=0$ of C_f by ones, using increasing index order for rows and columns. The normalized equation is $D_f r=e_0$, where e_0 denotes the coordinate vector for index zero.

Exact elimination and integer reduction give

$$\begin{aligned} &\det\left(2^{27} D_{\tilde{\phi}_0}\right) \equiv 92 \pmod{101}, \quad D_{\tilde{\phi}_0} \in \mathbb{Q}^{35\times 35}, \\ &\det\left(2^{25} D_{\tilde{\Phi}_1}\right) \equiv 75 \pmod{101}, \quad D_{\tilde{\Phi}_1} \in \mathbb{Q}^{33\times 33}. \end{aligned} \tag{51}$$

Both scaled matrices are integer matrices. Their nonzero determinants modulo 101 prove invertibility over $\mathbb{Q}$. Since the actual correlations satisfy both the recurrence and the normalization, they are the unique solutions of these systems. The rational solutions are also checked against every row of $C_f r = 0$, including the row replaced in D_f. Their absolute sums are approximately 18.5804751612 and 47.8964720425; the strict comparisons with 19 and 48 are made by exact integer cross multiplication. Positivity and the partition of unity of the cardinal splines give the other two bounds. Consequently,

$$B(B_4) = B(B_5) = 1, \quad B\left(\tilde{\phi}_0\right) < 19, \quad B\left(\tilde{\Phi}_1\right) < 48. \tag{52}$$

The supplementary rational module records the matrix dimensions, the modular determinants, the exact correlations and the positive rational margins. Theorem 3.1 and (52) now give (45) by duality. Finally, both transferred masks vanish at -1, to orders five and three. Since $\tau_-(\xi) = \mathrm{e}^{\mathrm{i}\xi}\tau(\xi)$, cancellation in the factorized product gives

$$\widehat{\tilde{\Phi}_1}(\xi) = \mathrm{e}^{-\mathrm{i}\xi}\tau(\xi)^3 \prod_{j\geq 1} R\left(\sin^2 \frac{\xi}{2^{j+1}}\right),$$

with the values at the removable zeros understood by continuity. The same product bound therefore gives decay with exponent $\alpha - 1 > 1/2$; B_5 decays faster. Theorem 4.3, and hence CDF's cross-scale criterion, applies. The orders at -1 give the stated wavelet moment counts. □

The Python scripts implementing the construction and certification procedures of Section 4.2 are available from the author upon request. They compute the four transferred filters and verify the spline example, the obstruction, the *D*24 enclosure, and the rational seed construction, including the Bernstein certificate and the separate cross-correlation and autocorrelation rank checks. The scripts use only the Python standard library. Their exact checks are separate from the floating-point illustrations. **Figure 6** shows why a numerical frequency plot is informative but cannot replace the strict inequality (47).

8. Scope and Conclusion

Table 5 summarizes the guarantees proved for the construction and for each specified example.

The central object of the 2009 note is an *algorithm that starts with a biorthogonal seed*; it does not depend on reversing its four illustrative plots. Spline transfer and related families have prior art [2]-[4] [7] [8]. Theorem 2.3 supplies an explicit L^2 qualification of the algorithm, while Theorem 6.1 shows on a complete algebraic mask class why filters alone do not certify its input. The rational extension in Theorem 7.1 supplies a concrete functional repair, with all its parameters and

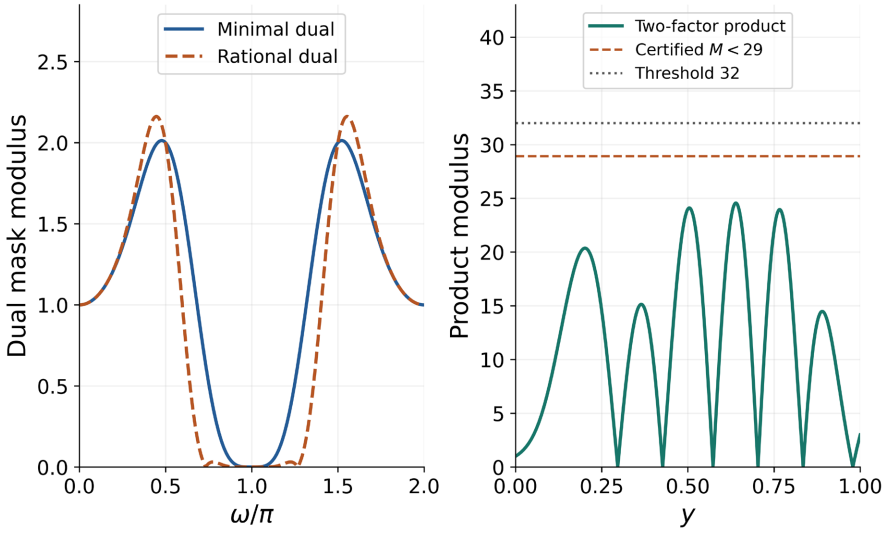

Figure 6. Degree-Minimal and extended order-four dual masks (left), and the two-level polynomial modulus of the rational extension (right). The plotted threshold 32 is proved by the rational Bernstein enclosure (47); sampled curves by themselves do not establish L^2 existence.

Table 5. Guarantees of the constructive method and status of examples.

Item	Established status
2009 construction [1] from an admissible seed	The recurrence (15) calculates the masks, and Procedure 4.1 certifies the functions and their translate Riesz bounds under the exact input test.
CDF B_2, $s=1$	Exact rational filter taps (**Table 2**), inverse, and optimal translate Riesz bounds 1 and 9/8 in (21).
Daubechies $D8$, $s=1$	Known Hölder regularity, order-four mask zero, translate bounds (24), and global dual Riesz bases.
Daubechies $D24$, $s=1,2$	Exact seed specification (25), L^2 functions, translate bounds (31), rational Fourier-decay certificate (28), and global dual Riesz bases.
Rational spline seed, $s=1$	Coefficients (41) with exact H^1, biorthogonality, rational Gram bounds, transferred constants $[1/48,1]$ and $[1,48]$, and global dual Riesz wavelet bases.
Degree-minimal spline complements	Theorem 10 proves a unique algebraic mask and no compact L^2 complement for every $m\geq 4$; the rational $m=4$ taps are in **Table 4**.
2009 illustrative plots	Their exact appearance is not inferred from the captions; their taps are not needed for forward construction from other specified seeds.
Global wavelet basis	Proved for the rational seed, $D8$, and both $D24$ transfers; no blanket claim for arbitrary seed pairs.

bounds specified. Classical factorization [5] [6], the earlier order-four observation [10], and the transfers of He/CDF are identified as precedents. The historical title describes a compactly supported kernel: the operator is not compact on $L^2(\mathbb{R})$

(Proposition 2.1). The rational and Daubechies executions close the functional and cross-scale gaps for specified transfers. The rational coefficients and their certified bounds are the particular design reported here; the general families and methods remain classical.

Sensitivity to input perturbations.

The Riesz bounds proved here concern expansions in the exactly specified scaling or wavelet families. They do not by themselves prove numerical robustness of the construction with respect to perturbations of the seed data or mask coefficients. Since $\left(T^*\right)^{-s}$ is unbounded on its L^2 range, no uniform estimate of the form $\|g_1-g_2\|_2 \le C\|f_1-f_2\|_2$ holds for general admissible data. Moreover, an arbitrarily small perturbation can destroy a required zero of $\hat{f}$ at a nonzero $2\pi n$, so that the perturbed datum has no L^2 inverse. There is nevertheless conditional stability: if f_1, f_2 are admissible and supported in a common interval of length L, Theorem 2.3 applied to their difference gives

$$\|g_1-g_2\|_2 \le \binom{\lceil L \rceil}{s} \left\| D^s\left(f_1-f_2\right)\right\|_2, \quad g_i = \left(T^*\right)^{-s} f_i. \tag{53}$$

This is control in a stronger data topology, subject to exact admissibility and a common support bound.

Rounding general mask coefficients may alter normalization, perfect reconstruction or the required zero multiplicities. A practical implementation should preserve these identities through a constrained parameterization and certify the strict inequalities by exact or interval arithmetic. The particular rational filters in Section 7 have dyadic coefficients exactly representable in binary double precision, but subsequent cascade and signal computations still incur floating-point errors. The present certificates establish exact existence and Riesz bounds; they do not provide a perturbation theorem for the map from filter coefficients to scaling functions, or a rounding-error analysis of a numerical implementation.

Acknowledgements

This work was supported by the ADEN-MED project (Adaptability to Extreme Events and Natural Risks—Application to the Mediterranean and Djibouti), funded by the Région Sud Provence-Alpes-Côte d'Azur under the AAP MEDCLIMAT "Natural Risks and Food Sovereignty"; the France 2030 Priority Research Program and Equipment (PEPR) Maths-Vives—Mathematics in Interactions, targeted project HYDRAUMATH (ANR-23-EXMA-007), operated by the French National Research Agency (ANR); the ANTARES project, funded by the ANR; and the PHAROS project (Monitoring Hydrodynamic Processes for Improved Adaptability to Oceanographic and Submergence Risks), funded by the Région Sud Provence-Alpes-Côte d'Azur under the AAP Océan et Mer.

Conflicts of Interest

The author declares no conflicts of interest regarding the publication of this paper.

References

[1] Ersoy, M. (2009) A Construction of Biorthogonal Wavelets with a Compact Operator. arXiv:0811.4716v2. https://arxiv.org/abs/0811.4716

[2] Cohen, A., Daubechies, I. and Feauveau, J.-C. (1992) Biorthogonal Bases of Compactly Supported Wavelets. *Communications on Pure and Applied Mathematics*, **45**, 485-560. https://doi.org/10.1002/cpa.3160450502

[3] Lemarié-Rieusset, P.G. (1992) Analyses multi-résolutions non orthogonales, commutation entre projecteurs et dérivation et ondelettes vecteurs à divergence nulle. *Revista Matemática Iberoamericana*, **8**, 221-237. https://doi.org/10.4171/rmi/123

[4] Unser, M. and Blu, T. (2003) Wavelet Theory Demystified. *IEEE Transactions on Signal Processing*, **51**, 470-483. https://doi.org/10.1109/tsp.2002.807000

[5] Ron, A. (1990) Factorization Theorems for Univariate Splines on Regular Grids. *Israel Journal of Mathematics*, **70**, 48-68. https://doi.org/10.1007/bf02807218

[6] Plonka, G. and Ron, A. (2001) A New Factorization Technique of the Matrix Mask of Univariate Refinable Functions. *Numerische Mathematik*, **87**, 555-595. https://doi.org/10.1007/pl00005424

[7] He, T. (2004) Biorthogonal Spline Type Wavelets. *Computers & Mathematics with Applications*, **48**, 1319-1334. https://doi.org/10.1016/j.camwa.2004.10.029

[8] He, T.-X. (2007) Construction of Biorthogonal B-Spline Type Wavelet Sequences with Certain Regularities. *Journal of Applied Functional Analysis*, **2**, 339-360. https://www.researchgate.net/publication/254630857_Construction_of_Biorthogonal_B-spline_Type_Wavelet_Sequences_with_Certain_Regularities

[9] Bittner, K. (2005) A New View on Biorthogonal Spline Wavelets. Preprint Series 2005-03, University of ULM. https://www.uni-ulm.de/fileadmin/website_uni_ulm/mawi/forschung/Preprint-Server/2005/spl_wave.pdf

[10] Dijkema, T.J. (2009) Adaptive Tensor Product Wavelet Methods for Solving PDEs. Ph.D. Thesis, Utrecht University. https://dspace.library.uu.nl/handle/1874/34169

[11] Daubechies, I. (1988) Orthonormal Bases of Compactly Supported Wavelets. *Communications on Pure and Applied Mathematics*, **41**, 909-996. https://doi.org/10.1002/cpa.3160410705

[12] Guglielmi, N. and Protasov, V.Y. (2016) Invariant Polytopes of Sets of Matrices with Application to Regularity of Wavelets and Subdivisions. *SIAM Journal on Matrix Analysis and Applications*, **37**, 18-52. https://doi.org/10.1137/15m1006945